DOI 10.1007/s10946-019-09797-1
Journal of Russian Laser Research, Volume 40, Number 3, May, 2019

IMPEDANCE SPECTROSCOPY OF POLYANILINE FILMS MODIFIED BY CARBON PARTICLES

Pavel Forsh,[1,2,3] **Alexey Tameev,**[4] **Alim Mazinov,**[5] **Konstantin Savin,**[1,3*]
Elizaveta Perchenko,[1] **Ekaterina Forsh,**[6] **Elena Guseva,**[6] **Alexey Shevchenko,**[5]
Oxana Gribkova,[4] **and Marine Tedoradze**[4]

[1]*Faculty of Physics, Lomonosov Moscow State University*
Vorob'evy Gory, Moscow 119991, Russia.

[2]*National Research Center "Kurchatov Institute"*
Academician Kurchatov Square, Moscow 123182, Russia

[3]*Lebedev Physical Institute, Russian Academy of Sciences*
Leninskii Prospect 53, Moscow 119991, Russia

[4]*Frumkin Institute of Physical Chemistry and Electrochemistry, Russian Academy of Sciences*
Leninskii Prospect 31, bld. 4, Moscow 199071, Russia

[5]*Vernadsky Crimean Federal University*
Prospect Vernadskogo 4, Simferopol 295007, Russia

[6]*Moscow Automobile and Road Construction State Technical University*
Leningradskii Prospect 64, Moscow 125319, Russia

*Corresponding author e-mail: savinkonstantin93 @ gmail.com

Abstract

We investigate the conductivity of a composite of PANI-PAMPSA and PANI-PAMPSA with carbon particles by impedance spectroscopy. We establish that the addition of carbon particles to the PANI-PAMPSA composite leads to a significant rise in the conductivity over the entire range of frequencies studied (from 10 Hz to 5 MHz). Such increase in conductivity is very important for using the PANI-PAMPSA composite in solar energy. We propose an equivalent electrical circuit of the samples investigated. At low frequencies, the conductivity dependence on frequency indicates the hopping mechanism of the charge carrier transport.

Keywords: polyaniline, carbon particles, impedance spectroscopy, current–voltage characteristics, frequency dependence of conductivity, hopping conductivity.

1. Introduction

Nowadays, composites based on polymers with inorganic particles have become more and more popular as materials for solar batteries. Solar cells based on such hybrid structures have a wide range of absorption due to the addition of inorganic particles. In addition, these elements have low cost due to the use of polymers. Polymers, such as P3HT, PANI, PCBM, MEH-PPV, PFB, and F8BT with CdSe, CdS, PbS, PbSe, ZnO, $CuInS_2$, and Si nanoparticles are often used for creation of these hybrid structures [1–9].

Polyaniline (PANI) is one of the most widely used conductive polymers. PANI complexes obtained in the presence of polysulfonic acids by oxidative aniline polymerization are water-dispersible complexes,

---

Manuscript submitted by the authors in English first on February 14, 2019 and in final form on April 10, 2019.

whose thin films possess electrical conductivity in the range of $10^{-3} - 10^{-1}\ \Omega^{-1} \cdot \mathrm{cm}^{-1}$ [10,11]. In particular, a complex consisting of PANI and poly-(2-acrylamido-2-methyl-1-propanesulfonic acid (PAMPSA) forms a stable aqueous dispersion along with exhibiting temporal stability of optical and electrical properties of thin films for at least two years [12]. In the PANI-PAMPSA films, the mobility of holes (major charge carriers) is of the order 1 $\mathrm{cm}^2 \cdot \mathrm{V}^{-1} \cdot \mathrm{s}^{-1}$, as is found from Hall-effect measurements [13]. The PANI-PAMPSA films in solar cells are used primarily as a transparent hole transport layer; therefore, a very important task is to increase their conductivity.

In this regard, the PANI-PAMPSA with carbon crystals (PANI-PAMPSA/C) is expected to be a promise material for fabrication of solar cells. The preparation technology of these materials is rather well developed, such as solar cells based on PANI layers [14]. Nevertheless, the charge carrier transport in PANI/C composites has been poorly explored. In this work, we study the conductivity of composites consisting of PANI-PAMPSA and carbon by impedance spectroscopy.

2. Materials and Method

PANI was synthesized in aqueous solution by oxidative aniline polymerization in the presence of PAMPSA (MW$\sim 2 \cdot 10^6$, 15 wt.% in H_2O, Sigma-Aldrich) [10,12]. Ammonium persulfate (analytical grade) was used as the oxidizer. The molar ratio of aniline to oxidizer was $1:1$ mol/mol, and the ratio of aniline to the sulfonic group of PAMPSA was $1:2$ mol/g-eq. sulfonic group. Acetone dispersion of carbon was prepared by sonication in a bath for 1.5 h followed by centrifugation (6000 rpm, 10 min) for removing particle aggregates. The carbon dispersion was added to the PANI-PAMPSA solution, and then the mixture was sonicated for 20 min to achieve a homogeneous distribution of the particles in the polymer.

A SEM image of carbon particles is shown in Fig. 1; the particles are graphite rods with a diameter of $\sim$10 μm and a length of hundreds of micrometers; agglomerates tens of micrometers in size are also observed. Thin films of the composite were prepared by drop casting the PANI-PAMPSA/C dispersion onto glass substrate and drying at room temperature. To study the electrical properties, aluminum contacts were vapor-deposited onto the surface of the films. Two distances were used between the contacts, namely, 1 and 0.1 mm. The conductivity was measured using a Keithley 6487 unit in the voltage range from -3 to 3 V. Frequency dependences of conductivity were measured by an HP 4192A impedance analyzer in the frequency range from 10 Hz to 5 MHz.

The Raman spectrum of PANI-PAMPSA films obtained using an Enspectr R532 spectrometer is shown in Fig. 2. The Raman spectrum exhibits a peak at 1,612 cm^{-1} (C–C stretching vibrations of the benzenoid ring), a band at 1,335 cm^{-1} (the C–N^+ vibration of the benzenoid ring), with a band of C–H stretching bending vibration of the benzenoid ring shifted to 1,172 cm^{-1}, and bands at 837 and 600 cm^{-1} corresponding to benzenoid ring deformations in polarons and bipolarons. The absence of a peak in the 1,462 cm^{-1} region corresponding to $\mathrm{C}=\mathrm{N}$ stretching vibration of the quinoid ring may indicate the fact that the polyaniline in the samples is predominantly in the nigraniline form.

3. Discussion and Conclusions

Figure 3 a shows the current–voltage characteristics for a pure PANI-PAMPSA (curve 1) and the PANI-PAMPSA/C with a distance between the contacts $l = 1$ mm (curve 2).

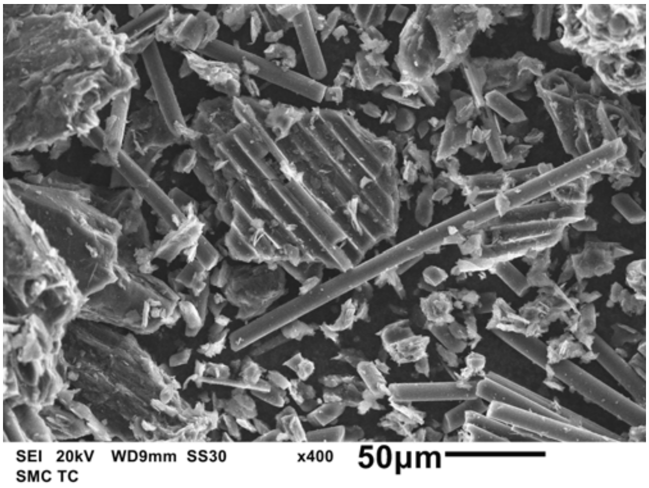

Fig. 1. SEM image of carbon particles.

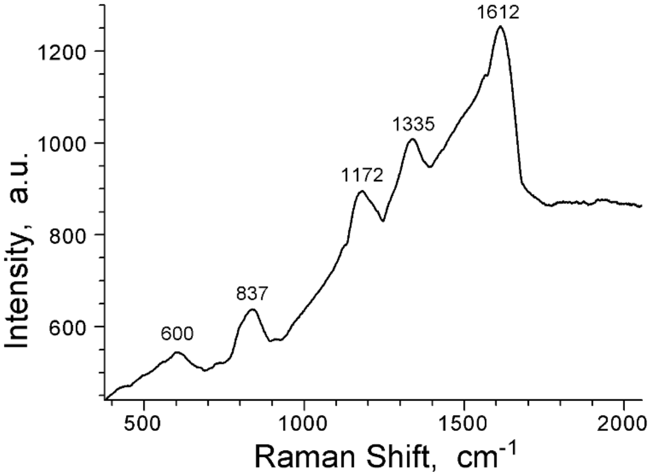

Fig. 2. Raman spectrum of PANI-PAMPSA films.

As one can see, all I-V characteristics are practically linear. At the same time, at a distance of $l = 0.1$ mm, the I-V characteristics become nonlinear. This may be explained by the existence of Schottky barriers on the boundaries between the sample and the electrical contacts. In the case of a large distance between the contacts, the resistance of the sample is sufficiently large and likely considerably exceeds the Schottky-barrier resistance, so the current–voltage characteristics in this case are linear (see Fig. 3 a). In the case of a small distance between the contacts, the resistance of the sample is comparable with the resistance of contacts, and the current–voltage characteristics become nonlinear. In order to exclude the influence of contacts on the measured characteristics, all measurements were carried out when the distance between contacts was equal to 1 mm.

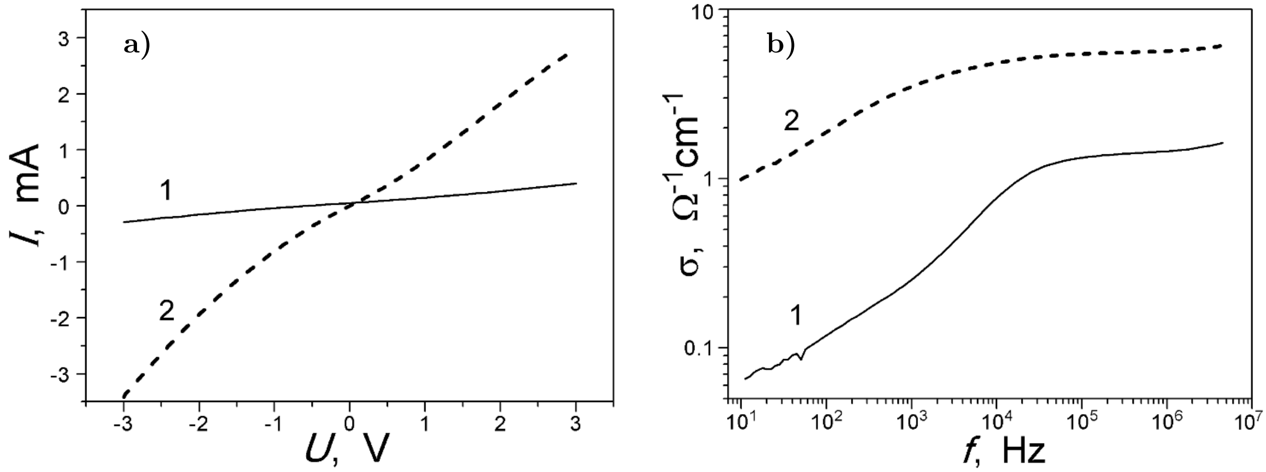

Fig. 3. Current–voltage characteristics (a) and frequency dependences of conductivity (b) for a pure PANI-PAMPSA (curve 1) and for the PANI-PAMPSA/C with a distance between the contacts equal to 1 mm (curve 2).

Frequency dependences of conductivity are presented on Fig. 3 b. As one can see, the dependences are similar for both samples but the conductivity of a sample with carbon particles is greater than that of the pure polymer sample for all frequencies studied.

A Cole-Cole plot for the PANI-PAMPSA/C is shown in Fig. 4 (a similar Cole-Cole plot was obtained for the pure PANI-PAMPSA). This diagram is often described by the equivalent circuit shown in Fig. 4 [15–18]. This equivalent circuit consists of two series-connected parallel RC circuits. Here, R1 and C1 represent the contribution of the electrode–sample interface to the resistance and the capacitance, and R2 and C2 represent the contribution to the resistance and capacitance arising from the grain boundaries. We should note that the contact resistance R1, which has no influence at the DC mode (with a large distance between the contacts), begins to appear on the alternating signal by shunting the resistance R2 by the capacitance C2 as the frequency increases (the capacitance decreases with frequency increase in accordance with $1/\omega C_2 \sim 1/\omega$, where $\omega = 2\pi$ is the cyclic frequency).

The impedance of this circuit can be written as follows:

$$Z = \frac{R_1 + R_2 + i\,\omega R_1 R_2 (C_1 + C_2)}{(1 + i\omega C_1 R_1)(1 + i\omega C_2 R_2)}, \tag{1}$$

with the real and imaginary parts of the impedance represented as

$$\operatorname{Re} Z = \frac{(R_1 + R_2)(1 - \omega^2 R_1 R_2 C_1 C_2) + \omega^2 R_1 R_2 (C_1 + C_2)(R_1 C_1 + R_2 C_2)}{(1 - \omega^2 R_1 R_2 C_1 C_2)^2 + (\omega R_1 C_1 + \omega R_2 C_2)^2}\,, \tag{2}$$

$$\operatorname{Im} Z = \frac{\omega R_1 R_2 (C_1 + C_2)(1 - \omega^2 R_1 R_2 C_1 C_2) - \omega (R_1 + R_2)(C_1 + C_2)(R_1 C_1 + R_2 C_2)}{(1 - \omega^2 R_1 R_2 C_1 C_2)^2 + (\omega R_1 C_1 + \omega R_2 C_2)^2}\,. \tag{3}$$

We present the Cole-Cole plot based on the proposed equivalent circuit by the solid curve in Fig. 4.

As Fig. 3 b shows, at low frequencies, the conductivities of both samples (pure PANI-PAMPSA and PANI-PAMPSA/C) increase with increase in frequency; the frequency dependences of conductivity can be approximated by the power law $\sigma \propto w^3$.

It is known that the power frequency dependence at $0 < s \leq 1$ is characteristic of a hopping conduction mechanism [19–25]. In particular, such law is observed in nanogranular metals and composites, such as polymer-matrix–metal particles [26–28]. According to this model, the coefficient s depends on frequency, as can be seen in Fig. 3 b. Considering the high polarizability of the polymer matrix and the conductivity of carbon particles, which is close to a semiconductor, it is quite possible to form C-C dipoles from charged particles, which corresponds to the given hopping model. In particular, this may be indicated by the nature of the conduction curves, which reach a constant value at high frequencies. The identical nature of the Cole-Cole diagrams and the frequency dependences of the conductivity for samples with and without carbon particles indicate that the introduction of particles does not change the conduction mechanism. We can assume that the introduction of carbon particles affects the probability of charge carrier hops.

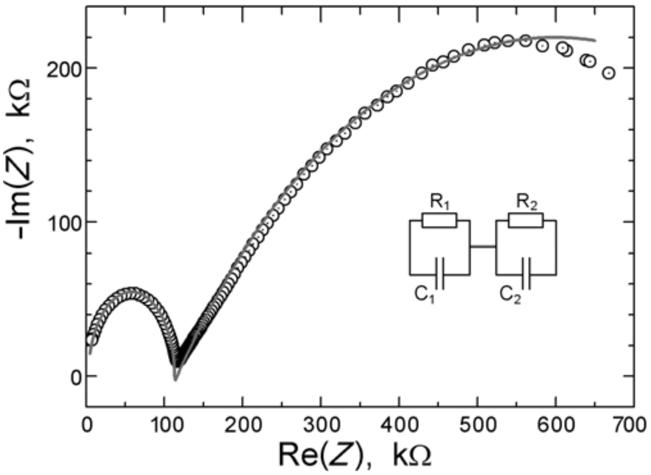

Fig. 4. The dependence of the imaginary part of the impedance on its real part for the PANI-PAMPSA/C. The inset shows a probable equivalent electric circuit.

4. Summary

In this paper, we studied the electrical properties of pure PANI-PAMPSA and PANI-PAMPSA with carbon particles and found that the I-V characteristics for both PANI-PAMPSA and PANI-PAMPSA/C samples with distance between contacts equal to 1 mm are practically linear. At the same time, when the distance between the contacts is equal to 0.1 mm, we have nonlinear current–voltage characteristics. This may be explained by the existence of Schottky barriers on the boundaries between the sample and the electrical contacts. In the case of a large distance between the contacts, the resistance of the sample is sufficiently large and likely considerably exceeds the Schottky-barrier resistance, so the current–voltage characteristics in this case are linear.

We demonstrated that the addition of carbon particles to the PANI-PAMPSA composite leads to the conductivity increase in the whole range of studied frequencies (from 10 Hz to 5 MHz), with the Cole-Cole plots for both PANI-PAMPSA and PANI-PAMPSA/C samples being similar. An equivalent electrical circuit that takes into account the resistance and capacitance of both the sample and electrical contacts is proposed.

An analysis of the frequency dependences of the conductivity of the studied samples is carried out based on the proposed equivalent circuit. We showed that in the low-frequency region the conductivity of the system is determined by the conductivity of the samples, i.e., of the PANI-PAMPSA or PANI-PAMPSA/C layers, and there is no contribution from the contacts. The frequency dependences of conductivity can be described by a power law, which is characteristic of the hopping conductivity. We assumed that the introduction of carbon particles into the PANI-PAMPSA matrix changes the jump probability of the charge carriers.

Acknowledgments

This work was supported by the Russian Foundation for Basic Research under Grant No. 18-29-23005.

References

1. N. Greenham, X. Peng, and A. Alivisatos, *Phys. Rev. B*, **54**, 17628 (1996).
2. W. U. Huynh, X. Peng, and A. P. Alivisatos, *Adv. Mater.*, **11**, 923 (1999).
3. W. U. Huynh, J. J. Dittmer, N. Teclemariam, et al., *Phys. Rev. B*, **67**, 115326 (2003).
4. E. Arici, N. S. Sariciftci, and D. Meissner, *Adv. Funct. Mater.*, **13**, 165 (2003).
5. S. A. McDonald, G. Konstantatos, S. Zhang, et al., *Nature Mater.*, **4**, 138 (2005).
6. D. Cui, J. Xu, T. Zhu, et al., *Appl. Phys. Lett.*, **88**, 183111 (2006).
7. W. J. Beek, M. M. Wienk, and R. A. Janssen, *Adv. Mater.*, **12**, 1009 (2004).
8. W. J. E. Beek, M. M. Wienk, and R. A. J. Janssen, *Adv. Funct. Mater.*, **16**, 1112 (2006).
9. K. M. Zaidan, H. F. Hussein, R. A. Talib, and A. K. Hassan, *Energy Procedia*, **6**, 85 (2011).
10. O. L. Gribkova, A. A. Nekrasov, M. Trchova, et al., *Polymer*, **52**, 2474 (2011).
11. O. D. Omelchenko, O. L. Gribkova, A. R. Tameev, et al., *Protect Met. Phys. Chem. Surf.*, **50**, 613 (2014).
12. O. D. Iakobson, O. L. Gribkova, A. A. Nekrasov, et al., *Prot. Met. Phys. Chem. Surf.*, **52**, 1005 (2016).
13. O. L. Gribkova, A. A. Nekrasov, V. A. Cabanova, et al., *Chem. Papers*, **72**, 1741 (2018).
14. O. D. Iakobson, O. L. Gribkova, A. R. Tameev, et al., *J. Ind. Eng. Chem.*, **65**, 390 (2018).
15. Shaker Ebrahim, *Polymer Sci.*, Ser. A, **53**, 1217 (2011).
16. C. H. Manathunga and V. P. S. Perera, in: *Annual Academic Sessions* (2013), p. 365.

17. P. A. Forsh, M. N. Martyshov, V. Yu. Timoshenko, and P. K. Kashkarov, *Phys. Status Solidi C*, **4**, 1981 (2007).
18. P. A. Forsh, M. N. Martyshov, V. Yu. Timoshenko, and P. K. Kashkarov, *Semiconductors*, **40**, 471 (2006).
19. M. H. Brodsky, *Amorphous Semiconductors*, Springer, Berlin, Heideberg, New York (1985), p. 118.
20. J. C. Dyre and T. B. Shroder, *Rev. Mod. Phys.*, **72**, 873 (2000).
21. A. K. Jonscher, *Nature*, **267**, 673 (1977).
22. A. R. Long, *Adv. Phys.*, **31**, 553 (1982).
23. J. C. Dyre, *Phys. Lett. A*, **108**, 457 (1985).
24. J. C. Dyre and T. B. Shroder, *Phys. Status Solidi B*, **230**, 5 (2002).
25. T. B. Shroder and J. C. Dyre, *Phys. Chem. Chem. Phys.*, **4**, 3173 (2002).
26. T. N. Koltunowicz, P. Zukowski, O. Boiko, et al., *J. Electron. Mater.*, **44**, 2260 (2015).
27. G. S. Psarras, *Composites*, Pt. A, **37**, 1545 (2006).
28. P. Zukowski, T. N. Koltunowicz, O. Boiko, et al., *Vacuum*, **120**, 37 (2015).